

Thermolysis of Free-Radical Initiators: *tert*-Butylazocumene and Its 1,3- and 1,4-Bisazo and 1,3,5-Trisazo Analogues

Paul S. Engel,* Li Pan, Yunming Ying, and Lawrence B. Alemany

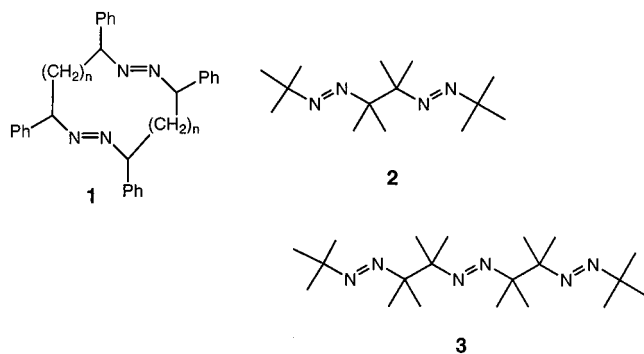
Contribution from the Department of Chemistry, Rice University, P.O. Box 1892, Houston, Texas 77251

Received November 9, 2000

Abstract: Four *tert*-butylazocumenes (**4–7**) were prepared from the corresponding cyanobenzenes, and their nitrogen evolution kinetics and products were analyzed. In combination with TEMPO, the simplest compound, *tert*-butylazocumene (**4**), shows promise as a “one-radical” initiator of styrene polymerization. The ABNO-trapped cumyl radical **29** is a particularly stable trialkylhydroxylamine, whose thermolysis half-life is 2.1 h at 150 °C. Taking advantage of this stability, we trapped the cumyl radical centers from **7** to afford tris adduct **32a**. While the behavior of the meta bisazoalkane **6** can be mostly predicted from that of **4**, the para isomer **5** exhibits both unusual products and kinetics, attributed to the formation of quinodimethane **33** via azo-containing radical **34**. In fact, flash vacuum pyrolysis of **5** allowed observation of the ¹H and ¹³C NMR spectra of **33**, whose persistence even at ambient temperature showed that this quinodimethane is far more stable than the parent **36**. Finally, evidence is presented that **7** is an initiator of star polymerization.

Azoalkanes are widely used initiators of free-radical polymerization.^{1–3} Depending on the substituents at the α -carbon, these compounds decompose thermally over a wide temperature range.⁴ Bifunctional initiators^{5–7} afford radicals that contain a latent initiator moiety that may become a polymer end group. Decomposition of such a polymer in the presence of additional monomer leaves the initiator core at the interior of a polymer chain.

A number of azo-containing bifunctional free-radical initiators have been reported,^{8,9} but several of the polyazoalkanes prepared thus far are ineffective. Thus, a macrocyclic bisazoalkane **1** made by Overberger¹⁰ is a poor initiator on account of rapid recombination of the biradical.^{11,12} Other bisazoalkanes such as **2**¹³ and **3**¹⁴ decompose via β -azo radicals that are too short-



lived to attack a monomer. However, if the azo groups are separated by a long enough chain, polyazoalkanes can serve as bifunctional initiators.^{9,15}

(1) Moad, G.; Solomon, D. H. *The Chemistry of Free Radical Polymerization*; Elsevier Science, Inc.: New York, 1995.

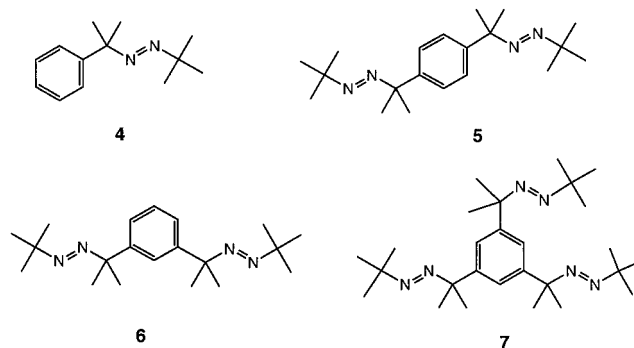
(2) Moad, G.; Solomon, D. H. In *Azo and Peroxy Initiators*; Moad, G., Solomon, D. H., Eds.; Pergamon Press: Oxford, 1989; Vol. 3, Chapter 8, pp 97–146.

(3) Takahashi, H.; Ueda, A.; Nagai, S. *J. Polym. Sci. A* **1997**, *35*, 69–76.

(4) Engel, P. S. *Chem. Rev.* **1980**, *80*, 99–150.

(5) Yoon, W. J.; Choi, K. Y. *J. Appl. Polym. Sci.* **1992**, *46*, 1353–1367.

In the present report, we describe the free-radical chemistry of initiators **4–7**. Azoalkanes **5–7** are new, but **4**¹⁶ and two



related compounds¹⁷ are already known. Mechanistic studies of **4** are lacking, despite the fact that this initiator affords two

(6) Hepuzer, Y.; Bektas, M.; Denizilgli, S.; Onen, A.; Yagci, Y. *Macromol. Rep.* **1993**, *A30*, 111–115.

(7) Gravert, D. J.; Datta, A.; Wentworth, P.; Janda, K. D. *J. Am. Chem. Soc.* **1998**, *120*, 9481–9493.

(8) Schulz, M.; West, G.; Ourk, S. *J. Prakt. Chem.* **1975**, *317*, 463–478.

(9) Sheppard, C. S. Symmetrical Trisazo Sequential Free Radical Initiators Having Two Different Azo Functions. Sheppard, C. S., Ed. U.S. Patent No. 3,868,359, 1975.

(10) Overberger, C. G.; Lapkin, M. *J. Am. Chem. Soc.* **1955**, *77*, 4651–4657.

(11) Biondic, M.; Giacobello, S.; Bassells, R. E.; Encinas, M. V.; Lissi, E. A. *J. Polym. Sci.* **1996**, *34*, 1941–1944.

(12) Kopecky, K. R.; Evani, S. *Can. J. Chem.* **1969**, *47*, 4041–4048.

(13) Engel, P. S.; Chen, Y.; Wang, C. *J. Am. Chem. Soc.* **1991**, *113*, 4355–4356.

(14) Engel, P. S.; Pan, L.; Whitmire, K. H.; Guzman-Jimenez, I.; Willcott, M. R.; Smith, W. B. *J. Org. Chem.* **2000**, *65*, 1016–1021.

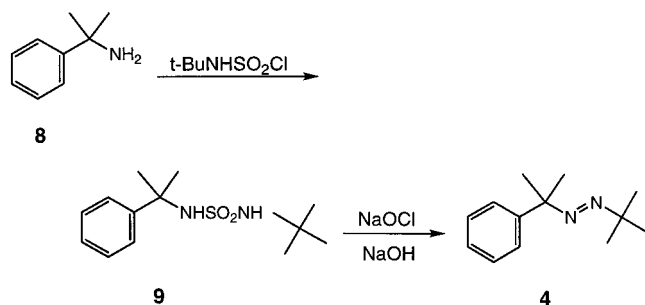
(15) Hill, J. W. Polymeric Azines, Hydrazonitriles, and Azonitriles. Hill, J. W., Ed. DuPont, U.S. Patent No. 2,556,876, 1951.

(16) MacLeay, R. E.; Sheppard, C. S. Unsymmetrical Azo and Hydrazo Compounds. MacLeay, R. E.; Sheppard, C. S., Eds. Canadian Patent 924,299, 1973.

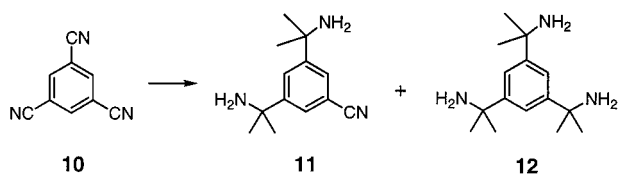
(17) Hinz, J.; Ruchardt, C. *Justus Liebigs Ann. Chem.* **1972**, *765*, 94–109.

well-studied radicals: cumyl^{18–20} and *tert*-butyl.^{21–23} The cross reactions of these radicals are described herein. Even though **5–7** decompose by sequential loss of azo groups, the resulting cumyl-type radicals have been trapped with stable nitroxides and with thiophenol. Pyrolysis of **5** yields the previously uncharacterized tetramethylquinodimethane **33**, while **7** is a probable initiator of star polymerization.

Synthesis of Azoalkanes 4–7. Treatment of cumylamine **8**^{24–26} with *tert*-butylsulfamyl chloride²⁷ afforded sulfamide **9**, which was oxidized with hypochlorite and base²⁸ to **4**. The



diamine precursors to **5** and **6** and triamine **12** were prepared by Ciganek's method²⁴ from 1,4-dicyanobenzene, 1,3-dicyanobenzene, and 1,3,5-tricyanobenzene **10**,²⁹ respectively, and were converted to **5–7** via the sulfamides. Because the organocerium reaction with **10** led to **11** plus **12**, the mixture was subjected



to $\text{CeCl}_3/\text{MeLi}$ again to complete the conversion to **12**; however, the final trisazoalkane **7** could not be purified as well as the bisazoalkanes.

Thermolysis Kinetics of 4. The kinetics of **4** and **5** could not be monitored by UV spectroscopy because thermolyzed solutions quickly developed greatly enhanced absorption in the region of 320 nm. Trisazoalkane **7** slowly formed a weaker but still intrusive absorber in the region of 360 nm. The cause of the interfering UV absorption was investigated by heating a 1-butanol solution of **4** for 5 min at 150 °C in a sealed tube equipped with both a 1-cm and a 2-mm UV cell. The formation of two short-wavelength bands was observed, one at 320 nm and a stronger one at 280 nm. Addition of sodium *n*-butoxide

(18) Nelsen, S. F.; Bartlett, P. D. *J. Am. Chem. Soc.* **1966**, *88*, 137–143.

(19) Leffler, J. E.; Zupancic, J. J. *J. Am. Chem. Soc.* **1980**, *102*, 259–267.

(20) Neuman, R. C.; Aldaheff, E. S. *J. Org. Chem.* **1970**, *35*, 3401–3405.

(21) Tanner, D. D.; Rahimi, R. M. *J. Am. Chem. Soc.* **1982**, *104*, 225–229.

(22) Blackham, A. U.; Eatough, N. L. *J. Am. Chem. Soc.* **1962**, *84*, 2922–2930.

(23) Tsentalovich, Y. P.; Fischer, H. *J. Chem. Soc. P2* **1994**, 729–733.

(24) Ciganek, E. *J. Org. Chem.* **1992**, *57*, 4521–4527.

(25) Cope, A. C.; Foster, T. T.; Towle, P. H. *J. Am. Chem. Soc.* **1949**, *71*, 3929–3934.

(26) Timberlake, J. W.; Alender, J.; Garner, A. W.; Hodges, M. L.; Ozmeral, C.; Szilagy, S. *J. Org. Chem.* **1981**, *46*, 2082–2089.

(27) Hendrickson, J. B.; Joffe, I. *J. Am. Chem. Soc.* **1973**, *95*, 4083–4084.

(28) Timberlake, J. W.; Hodges, M. L.; Betterton, K. *Synthesis* **1972**, 632–634.

(29) Bailey, A. S.; Henn, B. R.; Langdon, J. M. *Tetrahedron* **1963**, *19*, 161–167.

Table 1. Values of k_1 for **4–7** at Various Temperatures

$T, ^\circ\text{C}$	$10^4 k_1$ of x , s^{-1}				k_1 ratio of 4:5:6:7
	4 ^a	5 ^{b,c}	6 ^b	7 ^b	
101.37	1.434	3.635	3.209	4.188	1:2.54:2.24:2.92
106.68	2.665	7.475	5.921	7.865	1:2.80:2.22:2.95
110.74	4.111	12.80	9.353	12.59	1:3.11:2.28:3.06
114.79	6.258	21.65	14.62	19.93	1:3.46:2.37:3.18
119.52	10.54	39.45	24.35	33.67	1:3.75:2.31:3.20
125.49	19.18	82.47	45.56	64.14	1:4.30:2.38:3.34

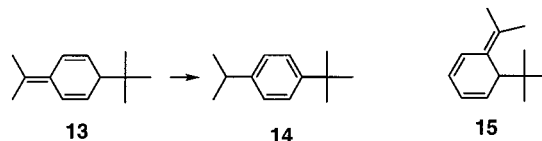
^a From experimental first-order nitrogen evolution data in decane. ^b Calculated from the activation parameters in Table 2 prior to rounding off. ^c From the ΔH^\ddagger and ΔS^\ddagger values in the third row of Table 2.

Table 2. Activation Parameters for k_1 of Compounds **4–7**

compd	ΔH^\ddagger_1 ^a	ΔS^\ddagger_1 , eu	R_1 ^b
4 ^c	31.1 ± 0.2	6.4 ± 0.5	0.9999
5 ^d	34.5 ± 0.4	16.1 ± 1.1	0.9998
5 ^e	37.6 ± 0.7	25.8 ± 1.7	0.9992
6 ^{e,f}	31.9 ± 0.1	10.2 ± 0.2	0.9998
7 ^g	32.8 ± 0.2	13.1 ± 1.6	0.9993

^a Kilocalories per mole. ^b Correlation coefficient of Eyring plot. ^c Taken directly from the experimental first-order plots. ^d Based on the 96.02–115.17 °C runs in Table 3, which gave linear first-order plots. ^e From all k_1 values in Table 3. ^f Based on only three temperatures. ^g From all k_1 values extracted from the N_2 evolution data using eq 2 (cf. Supporting Information).

caused only the 280-nm band to disappear, consistent with its assignment as the para quinoid recombination product **13** of *tert*-butyl radicals with cumyl. In support of this rationalization, the corresponding aromatized product **14** was found after thermolysis of **4** (see below). The 320-nm band may be from the ortho quinoid recombination product **15** analogous to that



previously seen in the photolysis of azocumene.^{30,31} The failure of the 320-nm band to disappear in base, even on heating at 150 °C for 10 min, and the fact that no GC/MS peak could be assigned to the corresponding aromatized compound, are consistent with an earlier report on azocumene.³¹

Because other analytical methods were deemed unsuitable, the decomposition kinetics of **4–7** were monitored by nitrogen evolution.³² The rate constants for **4** (cf. Table 1) were calculated from thermolysis data taken over at least 3.4 half-lives using the experimental infinity points, leading to the activation parameters included in Table 2.

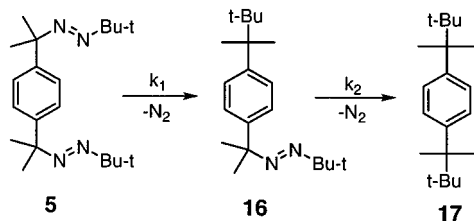
Thermolysis Kinetics of 5–7. Since nitrogen evolution was to be used for the kinetics of **5–7**, it was necessary to establish that N_2 was formed quantitatively. Samples of **6** and **7** were thermolyzed in benzene solution until all of the azoalkane had decomposed. Measurement of the nitrogen yield with a Töpler pump and gas buret gave 99.1% for **6** and 91.0% for **7**. The lower value for **7** is attributed to impurities in this compound.

Although the first-order nitrogen evolution plots for **4** were highly linear with correlation coefficients above 0.9993, those for **5–7** were distinctly curved. Before attempting to interpret

(30) Skinner, K. J.; Hochster, H. S.; McBride, J. M. *J. Am. Chem. Soc.* **1974**, *96*, 4301–4306.

(31) Neuman, R. C.; Amrich, M. J. *J. Org. Chem.* **1980**, *45*, 4629–4636.

(32) Billera, C. B.; Dunn, T. B.; Barry, D. A.; Engel, P. S. *J. Org. Chem.* **1998**, *63*, 9763–9768.

Scheme 1. Thermolysis Mechanism for Kinetic Simulation of **5**

these more complex kinetic data, we employed the program “Chemical Kinetics Simulator” (CKS) from IBM to generate nitrogen versus time curves for a simple scheme that might describe the thermolysis of **5** and **6** (see Scheme 1). One nitrogen molecule is lost in each of two sequential steps so the scheme for simulation is of the form $A \rightarrow B + N$ and $B \rightarrow N$ where A, B, and N represent **5**, **16**, and nitrogen, respectively. With $[A]_0 = 0.05$ M, the concentration of N generated by CKS was plotted as a first-order line using the expression $\ln[(0.1 - N)/0.1]$ versus time, where the 0.1 arises because each mole of A gives two of N. The value of k_1 was fixed arbitrarily at $2.0 \times 10^{-4} \text{ s}^{-1}$ while k_2 was varied from 5×10^{-5} to $1 \times 10^{-3} \text{ s}^{-1}$. As shown in Figure 1, when k_2 was $5 \times 10^{-5} \text{ s}^{-1}$, the “first order” plot fell more steeply at first than at later times, a curve shape similar to many of those found experimentally. When k_2 was set to half the value of k_1 , the plot was perfectly linear with a slope equal to k_2 . As k_2 increased further, the plots exhibited smaller initial slopes than at later times, inconsistent with any of our experimental data. When k_2 became quite rapid, the plot was again linear. The apparent rate constants (slopes) were always below k_1 , but they approached k_1 as k_2 was made faster, as expected (cf. Table 8, Supporting Information). These simulations suggested that treating the curved “first-order” plots as straight lines would be incorrect but that Scheme 1 might be a useful first approximation for the thermolysis of **5** and **6**.

To obtain values of k_1 , and k_2 from the experimental nitrogen evolution data, the coupled differential equations for the system $A \rightarrow B + N$ and $B \rightarrow N$ were solved analytically subject to the boundary conditions $A = A_0$, $B = N = 0$ at $t = 0$ and $A = B = 0$, $N = 2A_0$ at $t = \infty$. Representing the nitrogen pressure readings as P_0 , P , and P_∞ at times $= 0$, t , and ∞ , respectively, we derived eq 1.

$$\ln(P_\infty - P) = \ln\{2[A]_0 \exp(-k_1 t) + [A]_0 [k_1 / (k_2 - k_1)] [\exp(-k_1 t) - \exp(-k_2 t)]\} \quad (1)$$

where $[A]_0 = (P_\infty - P_0)/2$.

The experimental pressure versus time data were fitted to eq 1 using Kaleidagraph (Synergy Software) to extract values of k_1 and k_2 , which are summarized in Table 3 for **5** and **6**. Because the meta compound **6** was made late in this study, it was not investigated as thoroughly as the others, and only three temperatures were employed for kinetic measurements. The k_1 values in Table 3 were then plotted according to the Eyring equation to obtain the activation parameters included in Table 2. A similar treatment was applied to trisazoalkane **7** (cf. Supporting Information). The values of k_1 for **7** were fitted to the Eyring equation, yielding the activation parameters included in Table 2. To compare the k_1 values for **4–7**, we used the activation parameters in Table 2 to calculate the rate constant at each of the six temperatures (101.37–125.49 °C) of the rate measurements for **4**, with the results displayed in Table 1.

Product Studies. Thermolyzed solutions of **4** without scavenger and with thiophenol were analyzed by GC, giving

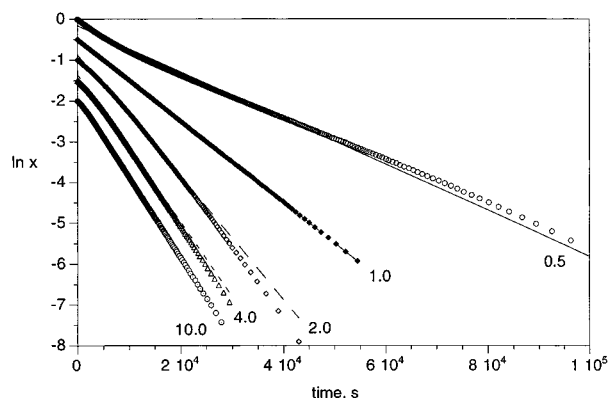
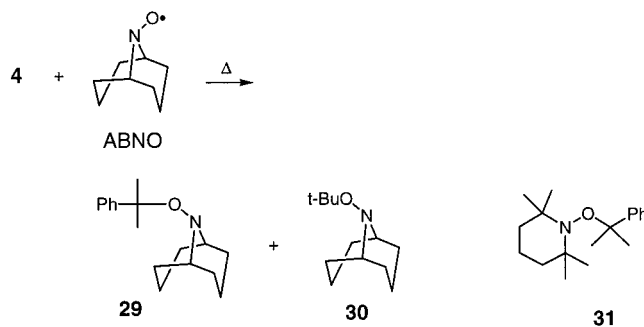


Figure 1. Simulated “first-order” plots of nitrogen evolution according to Scheme 1. $k_1 = 2 \times 10^{-4} \text{ s}^{-1}$ and k_2 varies from 0.5×10^{-4} to $10 \times 10^{-4} \text{ s}^{-1}$. $x = (0.1 - N)/0.1$. The straight lines are linear fits to the curves generated by CKS, yielding the values of m in Table 8 (cf. Supporting Information).

the results shown in Tables 4 and 5. Many of the products were identified with the aid of authentic samples, but in the more complex mixture lacking scavenger, two GC peaks were identified solely by mass spectrometry. The cumyl product balance was excellent (97%) in the presence of thiophenol but was only 66% without scavenger, where several products remain unidentified.

The products from bisazoalkanes **5** and **6** with PhSH are presented in Tables 6 and 7 while those from trisazoalkane **7** are shown in Table 9 (cf. Supporting Information). The complex mixture from **5** without scavenger was also analyzed (cf. Table 10, Supporting Information), but the aryl product balance was only 24%, and most of the structural assignments were based solely on GC/MS. The major product was 1,4-di-*tert*-heptylbenzene (**17**) while the second largest was *p*-isopropyl-*tert*-heptylbenzene (**23**).

Cage Effect of 4. The cage effect was determined by the excess scavenger technique.³³ We employed 9-azabicyclo[3.3.1]nonane-*N*-oxyl (ABNO)^{34,35} as the scavenger because **29** and **30** are thermally stable at 110 °C but the cumyl-TEMPO adduct **31** is not.^{36,37} A solution of **4** and ABNO in a 1-cm cell was



degassed and sealed and its UV spectrum recorded. After heating the solution at 110 °C for 5.4 half-lives, we found that the absorbance of ABNO had decreased to 51% of its original value, but heating for an additional 50 min produced no further change.

(33) Nelsen, S. F.; Bartlett, P. D. *J. Am. Chem. Soc.* **1966**, *88*, 143–149.

(34) Dupuyre, R. M.; Rassat, A. *Bull. Soc. Chim. Fr.* **1978**, 612–620.

(35) Mendenhall, G. D.; Ingold, K. U. *J. Am. Chem. Soc.* **1973**, *95*, 6395–6400.

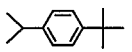
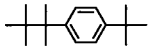
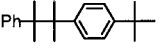
(36) Skene, W. G.; Belt, S. T.; Connolly, T. J.; Hahn, P.; Scaiano, J. C. *Macromolecules* **1998**, *31*, 9103–9105.

(37) Kothe, T.; Marque, S.; Martschke, R.; Popov, M.; Fischer, H. *J. Chem. Soc. P2* **1998**, 1553–1559.

Table 3. Thermolysis Rate Constants for Bisazoalkanes **5** and **6**

compd	<i>T</i> , °C	10 ⁴ <i>k</i> ₁ , s ⁻¹	10 ⁴ <i>k</i> ₂ , s ⁻¹
5	96.02	1.716	1.002
5	101.36	3.640	2.023
5	106.60	7.199	3.546
5	110.72	14.03	5.357
5	115.17	21.21	10.39
5	119.61	38.76	13.28
5	124.93	79.51	22.28
6	110.34	8.955	2.916
6	120.40	27.71	8.800
6	129.48	68.69	29.33

Table 4. Thermolysis Products of **4** without Radical Scavenger^a

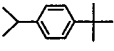
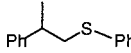
Product ^b	ret'n time, min ^c	moles/mol 4 ^d
isobutane ^e	1.69	0.118
isobutene ^e	1.71	0.0529
2,2,3,3-tetramethylbutane ^f	3.15	0.00700
cumene ^c	8.38	0.0951
α-methylstyrene ^c	9.85	0.00193
dodecane ^g	14.10	0.261
 14 ^e	14.82	0.00382
t-heptylbenzene ^h	15.55	0.194
 18 ⁱ	19.38 ^j	0.0130
bicumyl ^c	22.86	0.164
 19 ^j	25.75	0.0191

^a Conditions: 5.2 mg of **4** + 1.13 mg of dodecane in 0.25 mL of C₆D₆ heated at 112.9 °C for 8 h. ^b Superscript shows identification method. ^c GC retention time on HP-5 capillary column; see Experimental Section for details. ^d Calculated by assuming the same weight response factor for all compounds. ^e GC/MS compared with that of authentic sample. ^f GC/MS, NMR, and GC. ^g Internal standard. ^h Preparative GC, NMR, GC. ⁱ GC/MS. ^j Three unknowns were found at 19.69, 21.11, and 22.34 min.

The initial amount of **4** and the amount of ABNO consumed led to a cage effect of 18%. To quantify the thermal stability of **29**, its thermolysis in the presence of thiophenol was monitored by NMR, revealing the half-life at 150 °C to be 2.1 h.

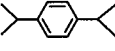
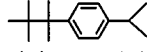
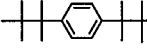
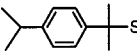
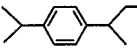
The Fate of Caged *tert*-Butyl–Cumyl Radical Pairs. Cage disproportionation of unlike radicals can occur in two possible directions. In the case of **4**, the products could be either isobutane plus α-methylstyrene (Scheme 2, path a) or isobutene plus cumene (path b). Unfortunately, none of these products can be readily used to quantify the two pathways in the presence of PhSH because the saturated compounds also arise by cage escape while the olefins are subject to attack by PhS[•].³⁸ To avoid this problem, we again took advantage of the thermal stability of **29** and subjected a thermolyzed solution of ABNO and **4** to GC analysis. ABNO surely captures all noncage radicals, so the relative yield of α-methylstyrene and cumene equals the uncorrected ratio (2.94:1) of path a to path b. Because cumyl–

Table 5. Thermolysis Products of **4** with PhSH^a

Product ^b	ret'n time, min ^c	moles/mol 4 ^d
isobutane ^e	1.60	0.639
cumene ^c	8.22	0.812
PhSH ^e	9.33	2.394
dodecane ^g	13.97	0.519
 14 ^e	14.37	0.0240
t-heptylbenzene ^h	15.32	0.0893
phenyl t-butyl sulfide ^e	15.56	0.00451
cumyl phenyl sulfide 20 ^e	21.86	0.0156
diphenyldisulfide ^c	22.86	0.340
 21 ^e	23.17	0.0262

^a Conditions: 22.2 mg of **4** + 9.6 mg of dodecane + 59.8 mg of PhSH in 2.0 mL of C₆D₆ heated at 112.9 °C for 8 h. ^{b–e,g,h} See footnotes to Table 4.

Table 6. Thermolysis Products of **5** with PhSH^a

Product ^b	ret'n time, min ^c	moles/mole 5 ^d
isobutane ^e	1.69	0.589
PhSH ^e	9.58	3.703
 22 ^e	13.75	0.487
dodecane ^g	14.09	0.373
phenyl- <i>t</i> -butyl sulfide ^c	15.79	0.00924
 23 ⁱ	18.91	0.127
 17 ⁱ	22.67	0.00030
diphenyldisulfide ^c	23.11	0.713
 24 ^e	24.64	0.0151
 25 ^e	26.03	0.0487

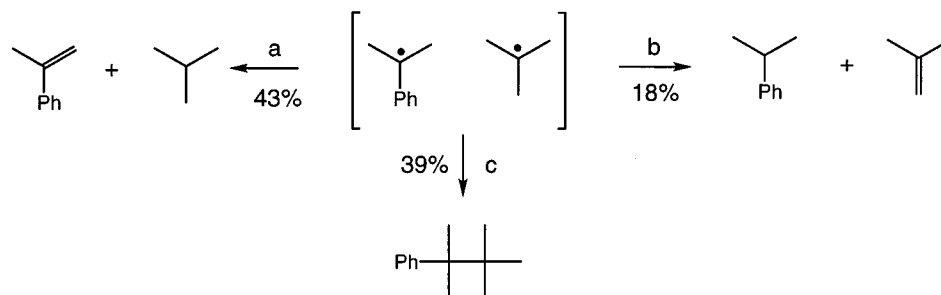
^a Conditions: 5.9 mg of **5** + 1.13 mg of dodecane + 15.7 mg of PhSH in 0.25 mL of C₆D₆ heated at 112.9 °C for 8 h. ^{b–e,g,i} See footnotes to Table 4.

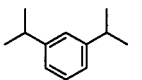
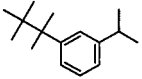
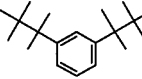
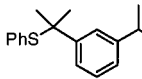
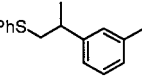
TEMPO pairs disproportionate to the extent of 5%,³⁹ a control experiment was required to determine how much α-methylstyrene arises from disproportionation of cumyl–ABNO pairs.

A solution of 0.031 M ABNO and 0.021 M azocumene (one ABNO per free cumyl radical, assuming a cage effect of 27%)³³ in C₆D₆ was heated in a sealed NMR tube at 90 °C for 10 min. The ¹H NMR area ratio of the α-methylstyrene olefin peaks to several characteristic two-proton multiplets of **29** was 0.086, which equals the disproportionation-to-recombination ratio of ABNO–cumyl radical pairs under these conditions. To correct for the fact that some of the α-methylstyrene from **4** + ABNO

(38) Engel, P. S.; He, S.-L.; Banks, J. T.; Ingold, K. U.; Luszyk, J. J. *Org. Chem.* **1997**, *62*, 1210–1214.

(39) Skene, W. G.; Scaiano, J. C.; Yap, G. P. A. *Macromolecules* **2000**, *33*, 3536–3542.

Scheme 2. Reactions of *tert*-Butyl–Cumyl Radical Pairs**Table 7.** Thermolysis of **6** with PhSH^a

Product ^b	ret'n time, min ^c	mole/mole 6 ^d
isobutane ^e	1.55	1.63
PhSH ^e	9.14	5.49
 26 ⁱ	12.96	0.620
n-dodecane ^g	13.74	1.40
phenyl- <i>t</i> -butyl sulfide ^e	15.37	0.00421
 27 ⁱ	17.92	0.128
 28 ⁱ	22.11	0.0104
diphenyldisulfide	22.65	0.817
 i	23.65	0.0178
 i	25.01	0.0408

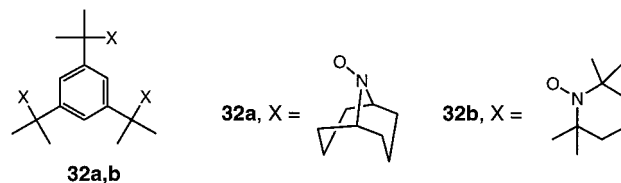
^a Conditions: 14.6 mg of **6** + 10.5 mg of dodecane + 51.5 mg of PhSH in 2.0 mL of C₆D₆ heated at 113 °C for 20 h. ^{b–e,g,i} See footnotes to Table 4.

arose by this pathway, we multiplied the relative area of **29** (6.60) by 0.086 and subtracted the result from 2.94 to obtain the relative amount (2.37) of α -methylstyrene that was actually formed by cage disproportionation. This correction is only approximate because the shape of the peak due to **29** indicated decomposition on the GC column.

tert-Heptylbenzene (relative yield 2.14) formed by cage recombination (Scheme 2, path c) was also observed in the GC trace of the ABNO + **4** thermolysis, but *p*-isopropyl-*tert*-butylbenzene **14** was hardly visible in this experiment. Since this α,p recombination product is present with PhSH scavenger, ABNO probably abstracts the reactive ring hydrogen from the semibenzene precursor **13** and captures the resulting substituted cumyl radical, leading to an ABNO adduct that did not survive GC. On the basis of the results of this ABNO experiment and the fact that nearly the same product composition was found for irradiation of **4** with TEMPO at 21 °C, we conclude that the percentage of radical pairs following paths a, b, and c in Scheme 2 is 43, 18, and 39%, respectively.

Because ABNO effectively trapped cumyl radicals to yield stable trialkylhydroxylamine **29**, we expected the same behavior

from **7**. Indeed, thermolysis of **7** with 3.4 equiv of ABNO at 124 °C for 35 min afforded **32a** in 18% yield.

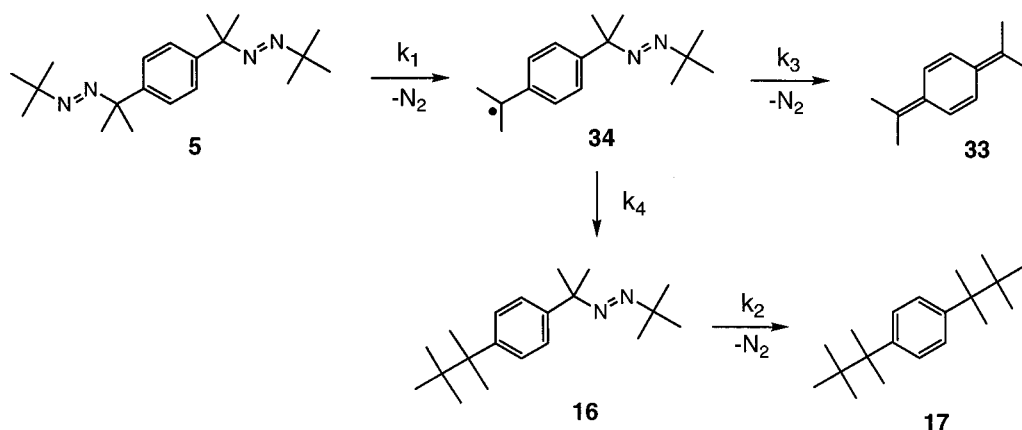


High-Temperature Pyrolysis of 5. We were astonished to discover that flash vacuum pyrolysis of **5** at ~ 350 °C afforded tetramethylquinodimethane **33** (cf. Scheme 3). The apparatus consisted of an addition funnel mounted atop a heated Pyrex column filled with glass beads. The pyrolysate was collected in a -78 °C trap attached to a sealable NMR tube. When a solution of **5** in toluene-*d*₈ was passed through this apparatus at 344 °C, the resulting solution showed encouraging ¹H NMR singlets at 1.67 and 6.66 ppm and a ¹³C peak at 123.84 ppm. The missing ¹³C signals were suspected to lie under the solvent peaks, so the pyrolysis was repeated in diglyme-*d*₁₄. This time all of the expected NMR signals of **33** were apparent. Monitoring these peaks as the solution aged at room temperature showed their contemporaneous disappearance over the course of 20 h. Solutions of **33** formed a highly insoluble polymer, a sample of which was isolated, washed, dried, and submitted for elemental analysis. The percent hydrogen was in excellent agreement with (C₁₂H₁₆)_n, but the carbon content was 4.8% low.

Discussion

The Eyring plots for k_1 of **5** and **6** were good straight lines, but those for k_2 were somewhat more scattered. While k_1 is associated specifically with deazotation of **5**, **16** is not the only azoalkane undergoing loss of a second nitrogen molecule (cf. Scheme 1). Thus, thermolysis of **5** gives radicals that disproportionate and recombine to produce other azo compounds whose thermolysis rates may differ from that of **16**. For this reason and because no consistent chemical explanation could be devised for the trends in k_2 , we shall interpret only k_1 . For **7**, although k_2 and k_3 gave surprisingly decent Eyring plots ($R = 0.9979$ and 0.9987 , respectively), they were not as good as those for k_1 , and it is unrealistic to expect meaningful values of three rate constants extracted from a simple curved line. Once again, we interpret only k_1 .

Based on statistics alone, k_1 of bisazoalkanes **5** and **6** should be twice that of monoazoalkane **4**. As seen in Table 1, the actual ratio for **6** is ~ 2.3 and is fairly constant over the experimental temperature range. Apparently, the meta azoalkyl substituent raises the ground-state energy of **6** and accelerates its decomposition. AM1 calculations indicated that the ground-state energy of **6** was higher by 0.3 kcal/mol than that of **5**, though this difference is not very meaningful at such a low level of theory.

Scheme 3. Proposed Thermolysis Mechanism of **5**

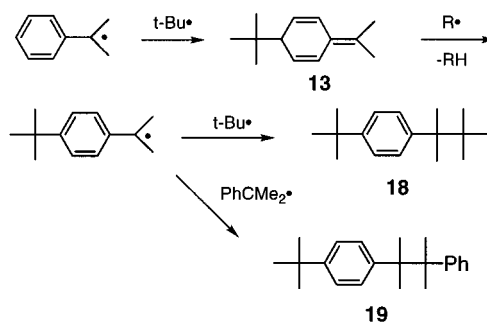
In view of the existing literature,^{40–43} we felt that there was little to be gained by further study of substituent effects in cumyl azo compounds. The situation for trisazoalkane **7** is similar to that of **6**. Statistically, we expect a rate enhancement of 3.0, but we find a slightly greater value (cf. Table 1), at least at the higher temperatures.

The k_1 value of **5** compared to **4** is even greater than that of the meta isomer **6**, and it rises more steeply at elevated temperatures. Apparently, the para azoalkyl group of **5** aids its thermolysis. Para methyl groups accelerate azocumene thermolysis by 46%, but *tert*-butyl has a much smaller effect.⁴⁰ On the other hand, para *tert*-butyl enhances the thermolysis rate of an azoepentane by 23%.⁴¹ The facts that the present compounds are unsymmetrical and that azoalkane thermolysis rates are subject to a polar effect⁴² might increase the influence of para alkyl groups.

An additional explanation for the fact that the rate constant of **5** is considerably larger than twice that of **4** and for the increase of the rate ratio with temperature is that some of the reaction leads to quinodimethane **33**. The lower temperature kinetic runs for **5** gave first-order plots that were much closer to linear than those from the 119.61 and 124.93 °C runs (cf. Tables 2 and 3). Nevertheless, the ΔH^\ddagger and ΔS^\ddagger values for **5** obtained from the 96.02–115.17 °C runs were higher than those for any other azo compound in Table 2. Still higher activation parameters were derived from k_1 values of all seven runs with **5**, suggesting that a new process, generation of **33**, comes into play at elevated temperatures.

Scheme 3 is an expanded version of Scheme 1 that includes formation of **33**. Using CKS, we set $k_1 = 2 \times 10^{-4} \text{ s}^{-1}$, $k_2 = 1 \times 10^{-4} \text{ s}^{-1}$, $k_4 = 10^9 \text{ s}^{-1}$, and $k_3 = 1 \times 10^8$ to $3 \times 10^8 \text{ s}^{-1}$. As k_3 became more competitive with k_4 , the apparent rate constant increased and the “first-order” plots curved in the direction found experimentally (cf. “0.5 line” in Figure 1). Deazotation of **34** (k_3) is surely a more activated process than recombination (k_4), and the resulting increase of the apparent rate constant with temperature could account for the high ΔH^\ddagger for **5** in Table 2.

Turning to the product distributions (Tables 4–7), we note that all of the identified products are easily rationalized as due to radical termination or hydrogen abstraction. The only unusual

Scheme 4. Mechanism for Formation of **18** and **19**

products from **4** are **18** and **19**, which must arise as shown in Scheme 4. Naturally such compounds are absent in the thiophenol scavenged runs; instead, we find sulfides formed by radical termination or addition to the isopropenyl group.

In Table 4, the yield of bicumyl is much higher than that of 2,2,3,3-tetramethylbutane, despite the fact that **4** produces cumyl and *tert*-butyl radicals in equal amounts. The self-termination rates of cumyl⁴⁴ and *tert*-butyl²³ radicals are $1.2 \times 10^9 \text{ s}^{-1}$ and $8.5 \times 10^9 \text{ M}^{-1} \text{ s}^{-1}$, respectively, and the disproportionation-to-recombination ratios are 0.054¹⁸ and 4.6.²¹ Since *tert*-butyl radicals terminate mainly by disproportionation ($k_d = 7.0 \times 10^9 \text{ M}^{-1} \text{ s}^{-1}$) and cumyl radicals mainly by recombination ($k_c = 1.1 \times 10^9 \text{ M}^{-1} \text{ s}^{-1}$), we calculate (using CKS) that the bicumyl-to-tetramethylbutane ratio should be 5.6:1. The actual ratio is considerably larger, but with a *tert*-butyl product balance of only 45% and a much greater yield of isobutane than isobutene, *tert*-butyl radicals are surely consumed by pathways such as hydrogen abstraction from semibenzene **13** (cf. Scheme 4). The lower steady-state concentration of *t*-Bu• decreases the amount of 2,2,3,3-tetramethylbutane.

In Table 5, the yield of the two cage recombination products *tert*-heptylbenzene and **14** corresponds to an α to para coupling ratio of 3.7, which is less than the values of 5.0 and 4.4 reported by McBride³⁰ and Neuman,³¹ respectively, for the recombination of cumyl radicals. Since cumyl is presumably larger than *tert*-butyl, the difference is in the wrong direction to be a steric effect. Instead, the considerably higher temperature required for thermolysis of **4** than azocumene may decrease the selectivity of recombination.

While the cage effect has been measured for a number of symmetrical azoalkanes,⁴⁵ there are few such reports for

(40) Shelton, J. R.; Liang, C. K.; Kovacic, P. *J. Am. Chem. Soc.* **1968**, *90*, 354–357.

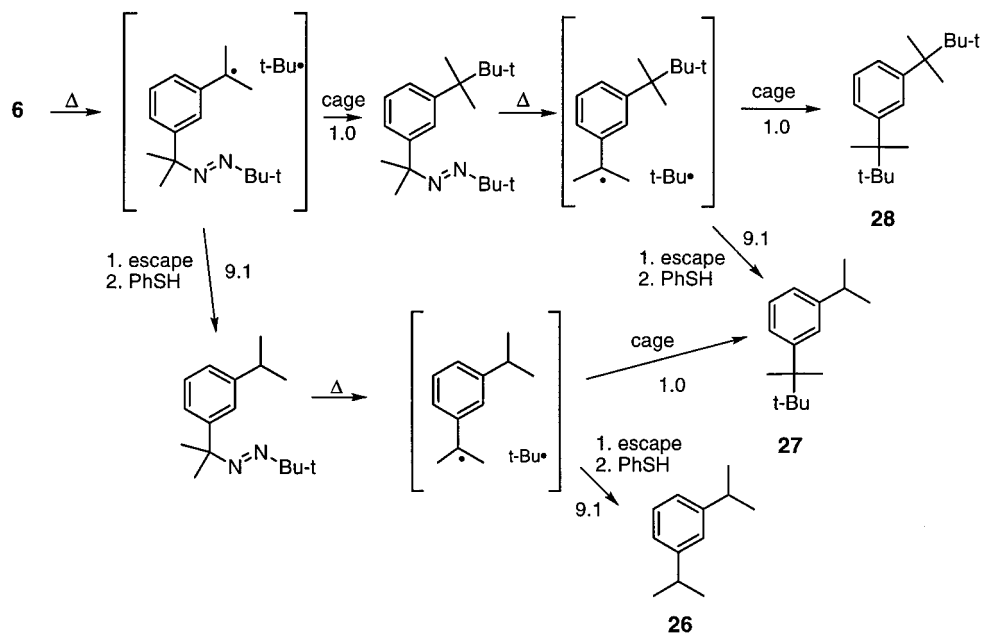
(41) Peyman, A.; Hickl, E.; Beckhaus, H.-D. *Chem. Ber.* **1987**, *120*, 713–725.

(42) Nau, W. M.; Harrer, H. M.; Adam, W. *J. Am. Chem. Soc.* **1994**, *116*, 10972–10982.

(43) Bandler, B. K.; Garner, A. W.; Hodges, M. L.; Timberlake, J. W. *J. Am. Chem. Soc.* **1975**, *97*, 5856–5862.

(44) Sobek, J.; Martschke, R.; Fischer, H. *J. Am. Chem. Soc.* **2001**, *123*, 2849–2857.

(45) Koenig, T.; Fischer, H. In *Cage Effects*; Koenig, T., Fischer, H., Eds.; Wiley: New York, 1973; Vol. 1, p 157.

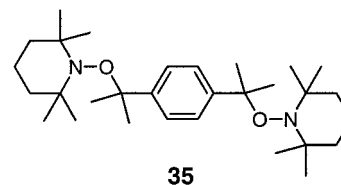
Scheme 5. Prediction of Product Ratio from **6**

unsymmetrical ones. The cage effect for azocumene at 40 °C in toluene is 27%³³ and that for photolysis of azo-*tert*-butane at 30 °C in benzene is 56%.²¹ We determined the cage effect of **4** from its product distribution in Table 5 and independently by the excess scavenger technique. The sum of PhCMe₂CMe₃ (*tert*-heptylbenzene) and **14** plus the secondary product of cage disproportionation, PhSCH₂CHPhMe (**21**), is 0.140 mmol (Table 5). Dividing this number by the sum of the cage and escape products (cumene and cumyl phenyl sulfide) gives a cage effect of 14%, in reasonable agreement with the value 18% obtained by the excess scavenger technique. In view of the relatively high temperature employed in our study of **4** and the activation energy of 1.3 kcal/mol for self-reaction of caged cumyl radicals,³³ the ~16% cage effect of **4** at 112.9 °C is entirely consistent with the 27% found for azocumene at 40 °C.

Analysis of the products of **4** in the presence of the stable nitroxyl radical ABNO gave the percentage of *tert*-butyl-cumyl radical pairs that follows each termination pathway. The 2.37:1 ratio of path a to path b (Scheme 2) shows the same trend as another unsymmetrical pair of radicals,³² suggesting that disproportionation favors the more stable olefin. This conclusion is opposite that reached by Gibian⁴⁶ for cross disproportionation of gas-phase alkyl radicals where the more substituted radical is the better hydrogen abstractor.

Determination of both the cage effect and the fate of *tert*-butyl-cumyl radical pairs relies on the thermal stability of **29**. We found that ΔG^\ddagger (150 °C) of **29** is 32.9 kcal/mol by monitoring its kinetics with PhSH to render C–O bond homolysis irreversible.⁴⁷ Because trialkylhydroxy amines have become important recently in the field of living free-radical polymerization,⁴⁸ several groups have studied their decomposition rates.^{36,37,49–51} Thermolysis of the cumyl-TEMPO adduct **31** proceeds under irreversible conditions with activation

parameters $E_a = 27.34$ kcal/mol and $\log A = 14.1$. Assuming that $\log A$ of **29** is also 14.1, we calculate an E_a of 35.1 kcal/mol, which is 7.8 kcal/mol higher than that of **31**. While the half-life of **31** is calculated to be 0.7 s at 150 °C, that of **29** is 2.1 h. This large difference is as expected from the 6.6 kcal/mol higher bond dissociation energy of ABNO–H (76.2 kcal/mol) than TEMPO–H (69.6 kcal/mol).⁵² Qualitatively, the high stability of **29** extends to the tris adduct **32a**, which we isolated from thermolysis of **7** with ABNO. Although **32a** is potentially an initiator of living free-radical star polymerization,^{53–55} the high temperature required for its thermolysis and the difficulty of preparing ABNO are drawbacks to its use (see, however, below). We succeeded in making the TEMPO analogue **32b** by irradiation of **7** with TEMPO, but on account of its lability, only a ¹H NMR spectrum was obtained. The chemical shifts were nevertheless comparable to those of **31**⁵⁶ and the para-bis adduct **35**, which we prepared in the same manner from **5**.



From the PhSH scavenged runs with **4** (Table 5), the ratio of cage escape to α recombination is 0.812:0.0893 = 9.1:1, which should hold true for **6** as well. In the presence of PhSH, **6** gave the product distribution shown in Table 7, with a benzene core balance of 81%. Stepwise cleavage as in Scheme 5 predicts that products **26**, **27**, and **28** will form in the ratio $(r/(r+1))^2 : 2r/(r+1) : 1/(r+1)^2$, where r is the ratio of cage escape to recombination. With $r = 9.1$, we calculate the **26:27:28** ratio

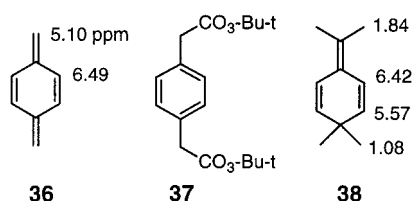
(46) Gibian, M. J.; Corley, R. C. *Chem. Rev.* **1973**, *73*, 441–464.
 (47) Engel, P. S.; Duan, S.; Arhancet, G. B. *J. Org. Chem.* **1997**, *62*, 3537–3541.
 (48) Hawker, C. J. *Acc. Chem. Res.* **1997**, *30*, 373–382.
 (49) Moad, G.; Rizzardo, E. *Macromolecules* **1995**, *28*, 8722–8728.
 (50) Ciriano, M. V.; Korth, H.-G.; van Scheppingen, W. B.; Mulder, P. *J. Am. Chem. Soc.* **1999**, *121*, 6375–6381.
 (51) Marque, S.; Le Mercier, C.; Tordo, P.; Fischer, H. *Macromolecules* **2000**, *33*, 4403–4410.

(52) Mahoney, L. R.; Mendenhall, G. D.; Ingold, K. U. *J. Am. Chem. Soc.* **1973**, *95*, 8610–8614.
 (53) Hawker, C. J. *Angew. Chem., Int. Ed. Engl.* **1995**, *34*, 1456–1459.
 (54) Zhou, D.; Yang, N.-L. *Polym. Prepr. (Am. Chem. Soc., Div. Polym. Chem.)* **1999**, 938–939.
 (55) Zhang, X.; Xia, J.; Matyjaszewski, K. *Macromolecules* **2000**, *33*, 2340–2345.
 (56) Connolly, T. J.; Baldovi, M. V.; Mohtat, N.; Scaiano, J. C. *Tetrahedron Lett.* **1996**, *37*, 4919–4922.

to be 1.0:0.22:0.012. From Table 7, we find that the actual values are 1.0:0.21:0.017, which are close to those predicted based on the product distribution from **4**. This agreement indicates that Scheme 5 adequately describes the thermolysis of **6**.

In contrast, attempts to rationalize the chemistry of **5** based on Scheme 5 lead to discrepancies. Starting from **5**, the observed ratio of **22:23:17** is 1.0:0.26:0.00060 (cf. Table 6). Two reasons for the low yield of **17** are the observed trapping of **34** by PhSH and the likelihood that some of **34** goes to **33** (Scheme 3), which escapes the solvent cage. The characteristic cloudiness due to the polymer of **33** was seen in the thermolysis of **5** but not in any of the other azo compounds in this study; moreover, the 24% GC product balance for **5** without thiophenol was unusually low. These discrepancies disappear if Scheme 3 is adopted. Generating **33** from **34** necessarily differs from the scheme proposed by Szwarc⁵⁷ for pyrolytic conversion of *p*-xylene to the parent quinodimethane **36**, where disproportionation of two benzylic radicals affords **36** plus *p*-xylene. On the other hand, Scheme 3 resembles the generation of **36** from α,α' -dichloro-*p*-xylene by laser photolysis, which also proceeds through a benzylic radical.⁵⁸ The reaction **34** \rightarrow **33**, whose exothermicity is calculated to be 11.5 kcal/mol, must compete with the rapid radical-radical reaction **34** + *t*-Bu \cdot at 113 °C. This is possible because deazotation of β -azo radicals is 10^{16} faster at 153.5 °C than that of azo-*tert*-butane,⁵⁹ a reaction whose calculated exothermicity is 29.3 kcal/mol. Despite the less favorable thermochemistry in the case of **34**, the rate could still be fast enough to compete with radical termination, especially under flash pyrolysis conditions (see below) because k_3 is unimolecular and k_4 is mostly bimolecular. Not only is **33** involved in the thermolysis of **5**, but it must be formed via **34** because thermolysis of **5** with PhSH yields *p*-diisopropylbenzene as the major product and it also yields some of the monoazoalkane formed when **34** abstracts hydrogen (cf. Supporting Information for an independent synthesis of 1-isopropyl-4-(2-*tert*-butylazo-2-propyl)benzene). *p*-Diisopropylbenzene could arise if **33** existed in the biradical form;⁶⁰ however, the parent quinodimethane **36** exhibits no ESR spectrum⁶¹ or NMR line broadening,⁶² arguing against much radical character.^{60,63} The fact that **36** has been trapped with TEMPO⁶⁴ can be taken to support the biradical structure, but since TEMPO adds to styrene,⁶⁵ it surely reacts with the quinoid form **36** as well. Thus, *p*-diisopropylbenzene is best explained by PhSH trapping of **34** followed by loss of the second azo group.

Unsubstituted quinodimethane **36** has been observed at low temperatures,⁶² and on warming,⁶¹ it forms a commercially useful polymer.^{66,67} Although heavily substituted analogues of **36** are stable, the only published work on **33** is a theoretical



calculation⁶⁸ and a surprising claim that it was made in 45% yield by pyrolysis of *p*-diisopropylbenzene.⁶⁹ Our successful

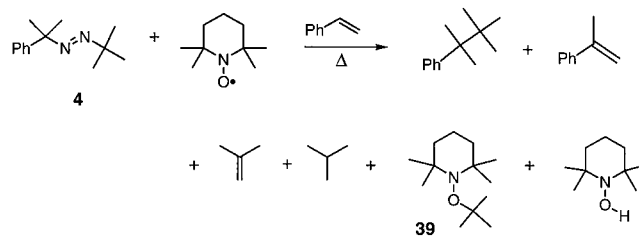
(57) Szwarc, M. *J. Chem. Phys.* **1951**, *16*, 128–136.

(58) Miranda, M. A.; Perez-Prieto, J.; Font-Sanchis, E.; Scaiano, J. C. *Chem. Commun.* **1998**, 1541–1542.

(59) Engel, P. S.; Wang, C.; Chen, Y.; Rüdhardt, C.; Beckhaus, H.-D. *J. Am. Chem. Soc.* **1993**, *115*, 65–74.

(60) Guihery, N.; Maynau, D.; Malrieu, J.-P. *Chem. Phys. Lett.* **1996**, *248*, 199–206.

Scheme 6. Thermolysis Products of **4** + TEMPO + Styrene



preparation of **33** from **5** stands in contrast to the pyrolysis of bisperester **37**, which gave no evidence for generation of **36**.⁷⁰

Since **33** disappeared over the course of 20 h at room temperature, it is far more stable than **36**, whose half-life toward polymerization is 21 h at -78 °C.⁶¹ The ^1H NMR spectrum of **33** in toluene- d_8 exhibited singlets at 1.67 and 6.66 ppm, which can be compared to the chemical shifts shown above of **36** in THF- d_6 ⁶² and **38** in CDCl_3 .⁷¹ All of the expected ^{13}C signals for **33** were observed, but we were unable to find ^{13}C spectra of **36** and **38** for comparison.

Azoalkanes 4 and 7 as Polymerization Initiators. The combination of azoalkanes **4–7** with TEMPO should constitute a unique system for living free-radical polymerization. In contrast to the systems studied previously,^{72–75} our azoalkanes produce two or more radicals of very different reactivity. In the case of **4**, both *tert*-butyl and cumyl radicals combine rapidly with TEMPO, but the cumyl-TEMPO adduct **31** is far more labile than the *tert*-butyl-TEMPO adduct **39** (Scheme 6). The *tert*-butyl radicals are rapidly removed from solution, in principle leaving only cumyl radicals to initiate polymerization. In effect, **4** becomes a “one-radical initiator”. A quantitative view of the system (**4**, TEMPO, styrene) reveals that, at 18 °C, the rate constant for *tert*-butyl plus TEMPO is $7.6 \times 10^8 \text{ M}^{-1} \text{ s}^{-1}$,⁷⁶ while that for *tert*-butyl plus styrene is only $1.1 \times 10^5 \text{ M}^{-1} \text{ s}^{-1}$.^{77,78} Even if the ratio of styrene to TEMPO is 150:1, 98% of the *tert*-butyl radicals will still react with TEMPO. Cumyl radicals combine with TEMPO at a rate of $1.2 \times 10^9 \text{ M}^{-1} \text{ s}^{-1}$ at 18 °C and with styrene at a rate of $1.2 \times 10^3 \text{ M}^{-1} \text{ s}^{-1}$.

(61) Errede, L. A.; Landrum, B. F. *J. Am. Chem. Soc.* **1957**, *79*, 4952–4955.

(62) Williams, D. J.; Pearson, J. M.; Levy, M. *J. Am. Chem. Soc.* **1970**, *92*, 1436–1438.

(63) Platz, M. S. *Quinodimethanes and Related Diradicals*; Wiley: New York, 1982.

(64) Li, I. Q.; Howell, B. A.; Koster, R. A.; Priddy, D. B. *Macromolecules* **1996**, *29*, 8554–8555.

(65) Connolly, T. J.; Scaiano, J. C. *Tetrahedron Lett.* **1997**, *38*, 1133–1136.

(66) Simon, P.; Mang, S.; Hasenhiindl, A.; Gronski, W.; Greiner, A. *Macromolecules* **1998**, *31*, 8775–8780.

(67) Loy, D. A.; Assink, R. A.; Jamison, G. M.; McNamara, W. F.; Prabakar, S.; Schnieder, D. A. *Macromolecules* **1995**, *28*, 5799–5803.

(68) Grand, A.; Jolibois, F.; Denis, J. P.; Dehalle, J. *Int. J. Quantum Chem.* **1997**, *61*, 689–697.

(69) Inoue, R.; Ichikawa, A. Pyrolysis of 1,4-diisopropylbenzene gives 1,4-diisopropylidene-cyclohexadiene. Japanese Patent 6521, 1962; *Chem. Abstr.* **1963**, *58*, 13819b.

(70) Lai, L.-F.; Tidwell, T. T. *J. Am. Chem. Soc.* **1977**, *99*, 1465–1470.

(71) Nelsen, S. F.; Teasley, M. F. *J. Org. Chem.* **1989**, *54*, 2667–2674.

(72) Hawker, C. J. *J. Am. Chem. Soc.* **1994**, *116*, 11185–11186.

(73) Howell, B. A.; Priddy, D. B.; Li, I. Q.; Smith, P. B.; Kastl, P. E. *Polym. Bull.* **1996**, *37*, 451.

(74) Kazmaier, P. M.; Daimon, K.; Georges, M. K.; Hamer, G. K.; Vergegin, R. P. N. *Macromolecules* **1997**, *30*, 2228–2231.

(75) Veregin, R. P. N.; Georges, M. K.; Hamer, G. K.; Kazmaier, P. M. *Macromolecules* **1995**, *28*, 4391–4398.

(76) Bowry, V. W.; Ingold, K. U. *J. Am. Chem. Soc.* **1992**, *114*, 4992–4996.

(77) Walbinder, M.; Wu, J.-Q.; Fischer, H. *Helv. Chim. Acta* **1995**, *78*, 910–924.

(78) Munger, K.; Fischer, H. *Int. J. Chem. Kinet.* **1985**, *17*, 809–829.

Although only 0.015% of cumyl radicals will add to styrene at our styrene/TEMPO ratio of 150:1, the addition is reversible at elevated temperatures, the essential feature of living free-radical polymerization.

To determine whether TEMPO actually prevents *tert*-butyl radicals from adding to styrene, we prepared a benzene solution of 0.030 M **4**, 4.0 M styrene, 0.0502 M TEMPO, and 0.0192 M undecane as internal standard. The degassed, sealed solution was heated at 120 °C for 3 h, opened, and immediately analyzed by GC. From the measured response factor of the GC stable **39**, we determined its concentration to be 0.0141 M, corresponding to 47% of the *tert*-butyl radicals. Of the remaining 53% of *tert*-butyl radicals, 40% were found as *tert*-heptylbenzene (10.5%) and as isobutane and isobutene (29.7%). This experiment was repeated with twice the amount of TEMPO, giving **39** (61%), *tert*-heptylbenzene (9.4%), and the C₄ gases (29.1%). The *tert*-butyl product balance of 87–100% shows that only a minor fraction of these radicals are available to attack styrene.

To be sure that **39** does not release *tert*-butyl radicals at 120 °C, we thermolyzed it separately in the presence of thiophenol,⁴⁷ similar to our study of **29**. A solution containing **39**, PhSH (4 equiv), and (MeO)₂CO (peak area standard) in C₆D₆ was heated in a 120.0 °C bath. The reaction was monitored by ¹H NMR of both starting material and products, yielding first-order plots with an average rate constant of $2.4 \times 10^{-5} \text{ s}^{-1}$. The formation of large amounts of isobutene suggests a concerted Cope-type elimination.^{50,79} Such a mechanism is consistent with the unusually low activation energy for thermolysis of **39** (33.7 kcal/mol from our observed rate constant and an assumed log A of 14.1) relative to the predicted value of 38.3 kcal/mol.⁵¹ Unlike the concerted process, even minor amounts of *tert*-butyl radicals from **39** could be problematic in the **4** + TEMPO initiator system; however, homolysis of **39** can be precluded by replacing *tert*-butyl with a bridgehead radical.

Preliminary experiments with **7** suggest that this trisazoalkane can be used to prepare star polymers, which are of interest because of their unique shape and their processing advantages.^{53,55} A solution of **7** and methyl methacrylate in benzene was heated to 122 °C for 20 min. The NMR spectrum of the purified polymer showed a broad NMR singlet at 7.0 ppm, and its UV spectrum was similar to that of 1,3,5-triisopropylbenzene. This result shows that the aromatic ring of **7** is present in the PMMA. In a second experiment, a styrene solution of **7**, TEMPO, benzoic acid,⁸⁰ and 2-fluoro-1-methylpyridinium *p*-toluenesulfonate (FMPTS)⁸¹ was degassed, sealed, and heated at 125 °C for 73 h. The concentration of TEMPO was chosen to react with all free radicals from **7**, using the 16% cage effect of **4** as a guideline. The isolated, reprecipitated polymer (69% yield) exhibited a molecular weight M_n of 13 050 and a polydispersity of 1.27. The GPC trace showed a major peak at molecular weight 14 750 with a shoulder at MW ~33 000, a behavior characteristic of dimerization of growing star polymer chains.⁸² Star polymers made from **7** contain no ester linkages such as those employed in the previous cases.^{53,54} While this structural feature is useful in making hydrolytically stable polymers,⁸³ it prevented us from characterizing the polymers

by analyzing their hydrolysis products, as was done so elegantly in the earlier studies.

Although further experiments would be required to fully establish the nature of the polymers initiated by **7**, several facts indicate that this trisazoalkane is a star polymer initiator: (1) the formation of 1,3,5-triisopropylbenzene as the major thermolysis product with PhSH (cf. Table 9, Supporting Information) and of **32a** with ABNO show that **7** generates three cumyl-type radicals on the same benzene ring, (2) the experiments with **4**, TEMPO, and styrene indicate that the cumyl radical is the major initiator, (3) PMMA prepared from **7** contains an aromatic ring, (4) a polymerization using **7**, styrene, TEMPO, and other additives yields a polymer of low polydispersity with the expected GPC peak shape, and (5) three-arm ester-linked initiators similar to **7** are known to generate star polymers.^{53,54}

In summary, we have shown that the first deazotation rate of *tert*-butylazocumenes **4–7** increases approximately statistically with the number of pendant azo groups. However, many of the “first-order” plots of nitrogen evolution are curved due to deviations from this statistical ratio and to deazotation of various secondary products such as **16**. The rate constant of **5** is higher than that of **6** and the product distribution of **5** is abnormal because it decomposes via an azo-containing radical **34** to the substituted quinonemethide **33**. Although it is far more stable than the parent quinonemethide, **33** polymerizes at room temperature over the course of ~20 h. *tert*-Butyl–cumyl radical pairs disproportionate in both possible directions, but the cumyl radical is a better H• donor than an acceptor. These radicals also couple at the para position 27% as much as at the α position. Cumyl radicals trapped by ABNO lead to **29**, which is a far more stable compound than the TEMPO adduct **31**. The system **4** plus TEMPO can act like a “one-radical” initiator because TEMPO traps the *tert*-butyl radical, while the thermally labile **31** is available to initiate the living free-radical polymerization of styrene. Finally, the weight of evidence indicates that trisazoalkane **7** is an initiator of star free-radical polymerization.

Experimental Section

General Methods. Anhydrous ether and THF were prepared by distillation from benzophenone ketyl. All NMR spectra were obtained in CDCl₃ unless otherwise specified. The analytical instruments have been described previously³² except for the Bruker Avance500 NMR spectrometer used to acquire the low-temperature ¹H and ¹³C NMR spectra of **33**. Gas chromatographic analyses employed an HP-5 capillary column: injector 200 °C, detector 250 °C, column 5 min at 50 °C, 10 °C/min to 250 °C, and hold 10 min. The mole/mole values listed in Tables 4–7, 9, and 10 were calculated using the following formula: $(A_p/A_{std})(W_{std})/(1/MW_i)(MW_{azo}/W_{azo})$, where A = GC peak area, W = weight (mg), MW = molecular weight, std = internal standard, x = product, and azo = azoalkane starting material.

Nitrogen Evolution Rate Measurements. A 2-mL flask containing a weighed amount of azo compound (13, 7, and 4 mmol for **4**, **5**, and **7**, respectively) and 1 mL of dodecane was connected to the gas evolution kinetics apparatus.³² The solution was degassed, backfilled with nitrogen, and immersed in a constant-temperature oil bath. The decomposition was monitored on a chart recorder, whose readings were taken manually and plugged into the computer program Kaleidagraph.

Cage Effect of **4 by the Excess Scavenger Technique.** A benzene solution of 0.094 M ABNO and 0.0282 M **4** was transferred into a 1-cm square tube with a 10/30 joint. After three cycles of freeze–pump–thaw, the tube was sealed under vacuum and the absorbance was determined to be 0.77 at 470 nm. The tube was then placed into a constant-temperature bath at 110 °C for 2.5 h, where $t_{1/2}$ of **4** is 28 min. After cooling to room temperature, the absorbance of ABNO was found to be 0.39. Heating the tube at 110 °C for the another 50 min led to essentially no change in UV absorbance. The decrease of ABNO

(79) We gratefully acknowledge helpful discussion with Professor Hanns Fischer, who has made similar observations.

(80) Georges, M. K.; Kee, R. A.; Veregin, R. P. N.; Hamer, G. K.; Kazmaier, P. M. *J. Phys. Org. Chem.* **1995**, *8*, 301–305.

(81) Odell, P. G.; Veregin, R. P. N.; Michalak, L. M.; Brousmiche, D.; Georges, M. K. *Macromolecules* **1995**, *28*, 3–8455.

(82) We thank Dr. Craig J. Hawker for pointing out the significance of the GPC peak shape.

(83) Quirk, R. P.; Tsai, Y. *Macromolecules* **1998**, *31*, 8016–8025.

absorbance showed that 49% of it had reacted, corresponding to an efficiency of 82% and a cage effect of 18%.

Thermolysis Rate of 29. A solution of 2.75 mg of azocumene and 2.2 mg of ABNO in 0.50 mL of benzene was degassed, sealed, and heated at 90 °C for 10 min to produce **29**. To the cooled solution was added 7.0 mg of thiophenol, 0.44 μL of dimethyl carbonate, and 0.71 μL of TMS as internal standards. The solution was degassed and sealed in an NMR tube, and the ^1H NMR spectrum was monitored periodically as the solution was heated in a 150 °C bath. The appearance of cumene, disappearance of **29**, and appearance of diphenyl disulfide gave scattered first-order plots due to spectral overlap, but the correlation coefficients were still above 0.985. The rate constant was determined to be $(9 \pm 1) \times 10^{-5} \text{ s}^{-1}$.

Generation of 33 by Pyrolysis of 5. The homemade apparatus consisted of a pressure equalized addition funnel atop a Pyrex column (8 cm \times 2 cm) filled with Pyrex beads and wrapped with a heating tape. A platinum thermometer inserted into a slanted well in the pyrolysis tube served to monitor the temperature. The pyrolysis tube was connected via a ground-glass joint to a U-shaped trap with a medium wall NMR tube attached at the bottom. Finally, the trap was connected to a vacuum pump via a -196 °C U-shaped cold trap. Solutions of **5** in toluene- d_8 or diglyme- d_{14} were slowly added onto the column under vacuum, and the collected material was allowed to melt into the NMR tube, which was then sealed. After pyrolysis, the walls of the U-trap and its attached NMR tube were covered with unreacted **5** and polymer from **33**. For **33** in diglyme- d_{14} , the ^1H NMR spectrum consisted of singlets at 1.89 (12H) and 6.59 ppm (4H) while the ^{13}C NMR spectrum showed peaks at 20.359, 123.913, 128.614, and 129.349 ppm.

Trapping of Radical 34. A solution of thiophenol (22 mg, 4 equiv.) and **5** (16.5 mg) in 0.2 mL of benzene was degassed, sealed, and heated at 115 °C for 8 min. The trapped monoazo product, 1-isopropyl-4-(2-*tert*-butylazo-2-propyl)benzene, was isolated by preparative TLC (or HPLC) using hexane as eluent. The NMR spectrum of this isolated product matched that of the independently synthesized compound (cf. Supporting Information).

Polymerization of PMMA by 7. Freshly distilled methyl methacrylate (0.5 mL) and 22.8 mg of **7** were dissolved in 4.5 mL of benzene. After three freeze–pump–thaw cycles, the tube was sealed and immersed in a 122 °C bath for 20 min. The tube was broken, and the polymer was precipitated with 30 mL of methanol. After filtration, the polymer was redissolved in 5 mL of benzene and reprecipitated with 30 mL of methanol. This process was repeated three times to remove low molecular weight material. The yield of PMMA was 62 mg or 12%. The UV spectrum exhibited a λ_{max} of 256 nm, and the ^1H NMR spectrum showed a broad singlet at 6.96 ppm among other, much stronger peaks.

Polymerization of Styrene by 7. A solution of 0.0143 M **7**, 0.0143 M benzoic acid, 0.00715 M FMPTS, and 0.0755 M TEMPO was degassed, sealed, and heated at 125 °C for 73 h. The polymer was isolated, dissolved in benzene, and reprecipitated with methanol three times. The percent conversion was determined by weighing and the molecular weight by GPC.

Acknowledgment. We thank the National Science Foundation and the Robert A. Welch Foundation for financial support. We also thank the NSF for funding the purchase of the 500-MHz NMR spectrometer (CHE-9708178). Finally, we are grateful to Professor Antonios G. Mikos for use of his gel permeation chromatograph.

Supporting Information Available: A kinetic treatment for thermolysis of **7**, synthetic details for all compounds, Table 8 containing the numerical values for Figure 1, Table 9 giving thermolysis products of **7** with PhSH, and Table 10 giving the thermolysis products of **5** without radical scavenger. This material is available free of charge via the Internet at <http://pubs.acs.org>.

JA003914U